All-purpose cell and module architecture for low-irradiance and concentrator applications

Tobias Fellmeth, Matthieu Ebert, Raphael Efinger, Ingrid Hädrich, Florian Clement, Ulrich Eitner & Daniel Biro,
Fraunhofer Institute for Solar Energy Systems (ISE), Freiburg, Germany

ABSTRACT

The combination of metal-wrap-through technology with a unit cell design, referred to as *AP-MWT architecture*, is proposed for the purpose of operating under low and concentrated irradiance. On the illuminated side, the negative polarity is electrically separated by using an emitter window surrounding the perimeter of each unit cell. The final functioning silicon-based device consists of an arbitrary amount of unit cells with perimeter dimensions ranging from 1cm × 2.25cm to 14cm × 13.5cm. The Czochralski-based bulk material, as well as the assembly approach, conforms with state-of-the-art industrially feasible technologies. For irradiances corresponding to 1 and 10 suns, median efficiencies of 19.8% and 20.9% and top efficiencies of 20.2% and 21.0% have been achieved. Thanks to the flexibility in size, interconnection and irradiance, a wide range of current–voltage ratios are covered, providing customized solutions beyond the conventional flat-panel market.

Introduction

The majority of silicon-based solar cells today are designed to operate under terrestrial sunlight in a flat-panel module [1]. For this reason, the IEC consortium offers a guideline for standard testing conditions (STC) [2], in which (among other testing conditions) a perpendicular irradiance of 1000W/m^2 is stipulated. Testing at different irradiances becomes a necessity when operational conditions vary from normal exposure to sunlight. This is the case for concentrator solar cells and for cells designed for operation under low irradiance conditions, for example indoor applications. The dimensionless concentration factor C defines the fraction of irradiance E, relative to the reference irradiance of E_{ref} = 1000W/m^2 at STC, at which the current–voltage characteristics (I-V curve) are recorded. For $C > 1$, concentration conditions apply, whereas for $C < 1$, the so-called *low-light* or *low-irradiance* conditions prevail.

Concentrator solar cells are designed to operate under enhanced irradiance ($C > 1$), typically within systems that contain an optical set-

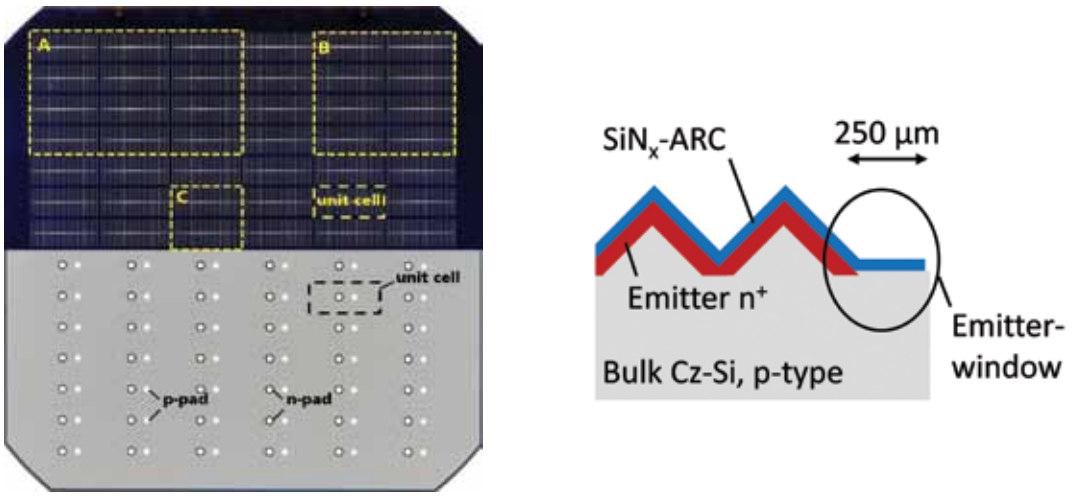

Figure 1. (a) Front (top) and rear (bottom) views of an AP-MWT wafer of the first generation, with edge lengths of 15.6cm, consisting of 84 solar cells called *unit cells*. The indicated examples A, B and C represent possible formats of a final cell, consisting of different numbers of unit cells of size 1cm × 2.25cm. In this case, the front-grid metallization is optimized for C = 10; the grid is adapted according to the respective irradiance. (b) Schematic cross section of the physical edge of an AP-MWT cell. The n$^+$ region is not extended to the edges, leaving an embedded emitter with the purpose of reducing edge recombination. Particularly for low light and small cell dimensions, the impact of edge recombination increases.

up which focuses the light onto a photovoltaically active element called the *receiver* [3]. The reduction in size of the solar cell, which is inversely proportional to the concentration factor, offers the potential for cost reductions, provided that all other system components are cost effective. Furthermore, the concentrator application allows higher cell efficiencies, mainly because of the logarithmic increase in open-circuit voltage V_{oc} [4] with concentration.

Silicon-based concentrator solar cells have been widely investigated in the past, generally using devices with the external polarities located on both sides or using back-contact back-junction (BCBJ) technology, in which the emitter and both external polarities are located on the rear side. For the former, the laser-grooved buried contact technology patented by the UNSW [5] and fabricated by BP Solar [6] represents an example that has been successfully introduced in manufacturing, which was assessed by the Euclides project [7]. The concentrator BCBJ cell was mainly investigated in the late 1970s and 1980s, resulting in the independently confirmed world-record efficiency of 27.6% [8] for a silicon solar cell. Only recently, SunPower Corporation modified their BCBJ cells to operate under an optical concentration of around 7 suns [9].

Low-irradiance conditions occur indoors and are associated with sensor technology or building-integrated solutions; these conditions can even occur outdoors in the case of mobile solutions in which the PV elements are mostly misaligned with the sun. Currently, the main solar cell supply for low-light applications comes from conventional solar cells being cut into smaller pieces, presenting the negative polarity on the illuminated side and the positive polarity on the rear.

Both concentrator and low-irradiance types of application share the need for flexible solutions in terms of their current–voltage ratios and perimeter dimensions. In the case of concentrator applications, a low current (I) device is desirable: resistive losses, which are proportional to I^2, are reduced. Low-light applications need high voltages and are often restricted to certain dimensions that are far below the standard wafer sizes of 5″ or 6″.

Fraunhofer ISE is therefore introducing a multipurpose silicon-based back-contacted solar cell architecture for use in a variety of bias light conditions. The cell front metal grid and perimeter dimensions are readily adaptable.

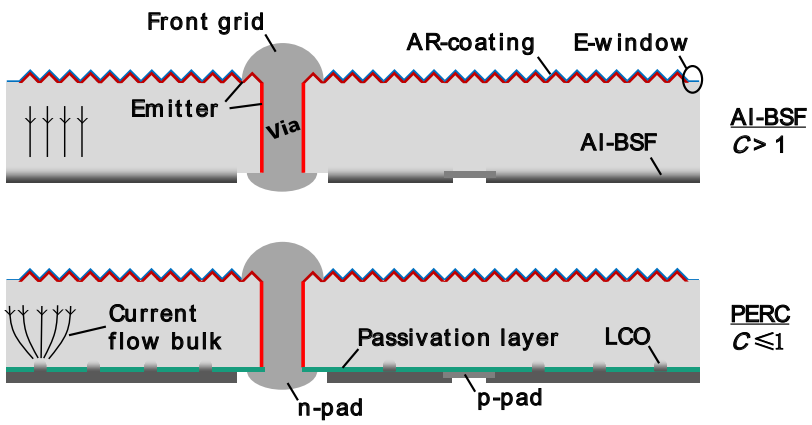

Figure 2. The AP-MWT architecture, featuring PERC technology (bottom), exhibits local contact openings (LCO), which substantially reduce the contacted fraction, leading to a low surface recombination velocity. In contrast, the full-area Al-BSF technology offers a low resistive solution, avoiding spreading resistance [12] in the bulk. For both approaches, the current flow towards the rear metal contact is indicated.

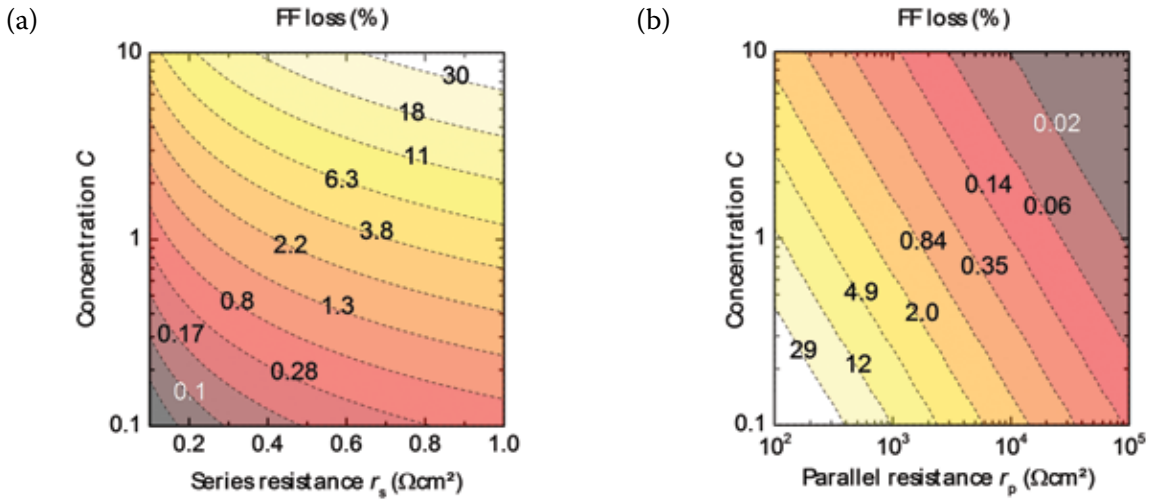

Figure 3. Regime shifts as a function of the concentration factor *C*, where *FF* losses are dominated by (a) series resistance, or (b) parallel resistance. Constant input parameters for the one-diode model: photo-generated current density at 1 sun j_{ph} = 37mA/cm²; j_{01} = 700fA/cm²; r_p = 0 in (a); r_s = 0 in (b). The impact of a second diode j_{02}, which corresponds to the behaviour similar to that of a parallel resistance reducing mainly the *FF*, is not shown.

The approach

Metal-wrap-through (MWT) [10] technology is combined with a flexible unit cell design, capable of producing an MWT device with dimensions between 1cm × 2.25cm and 14cm × 13.5cm, for operation between C = 0.1 and C = 25. This design will be referred to as *all-purpose MWT* (AP-MWT).

Fig. 1 shows the front and rear sides of an AP-MWT solar cell, illustrated on a 15.6cm semi-square monocrystalline wafer. The approach offers flexible sizes, indicated by the examples A to C, each consisting of a different number of unit cells. Each unit cell provides two solder pads for external contacting. The emitter of each unit cell is electrically separated by means of a 0.25mm-wide emitter window around the cell's perimeter, which reduces edge recombination when cut out of the wafer. As a result of the process sequence, the small perimeter area does not have any texture. On account of being MWT technology, both external polarities are located on the rear side, allowing an advanced interconnection in terms of exploiting the whole cell

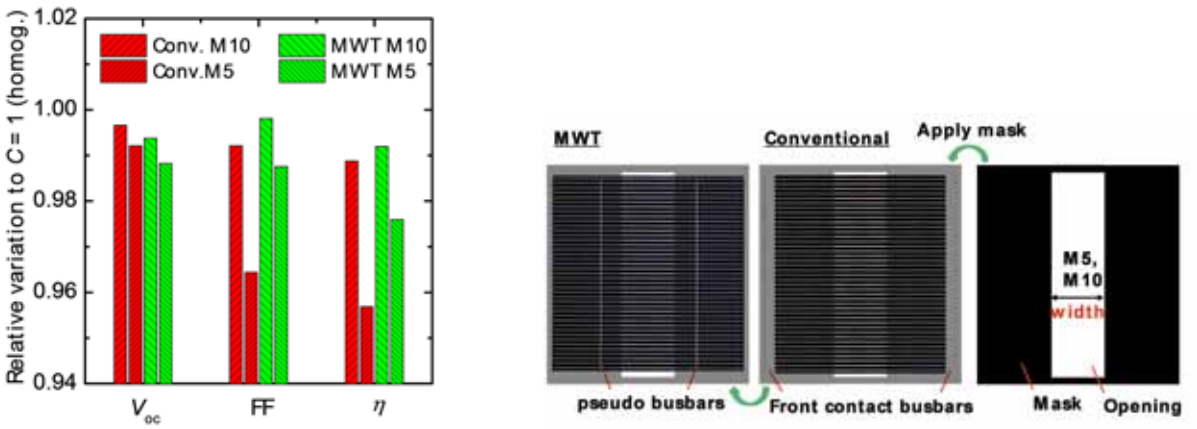

Figure 4. Sensitivity analysis as a result of applying a mask with different aperture widths of M5 = 5mm and M10 = 10mm. The unity reference represents a homogeneous irradiance of C = 1. After applying a mask, irradiance is increased until the short-circuit current corresponds to that for the homogeneous, C = 1, case.

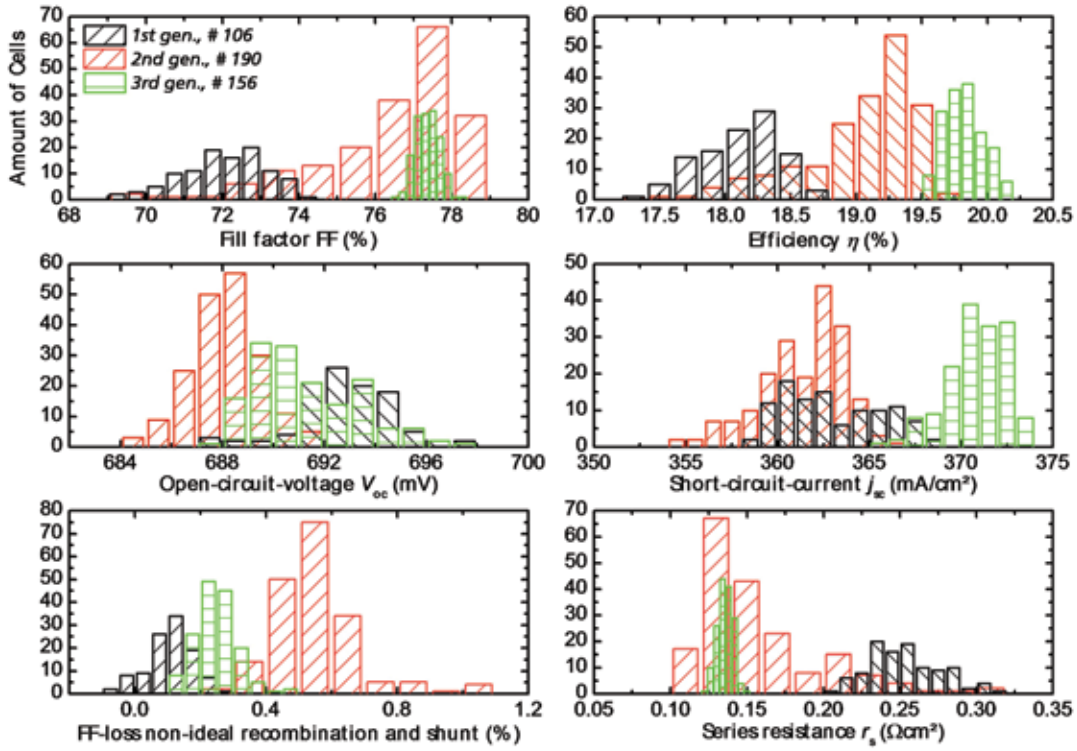

Figure 5. Evolution of *I-V* curve parameters for first, second and third generation cells. The *I-V* curves are recorded in the individualized cell state, whereas the dimensions of the first and second generations correspond to format A, and the third generation to format B (see Fig. 1). A clear trend towards higher mean and peak efficiencies is evident, but, at the same time, the variation is significantly reduced. Conditions: C = 10 (E_{in} = 10kW/m²), T = 25°C, spectrum AM1.5g, stabilized.

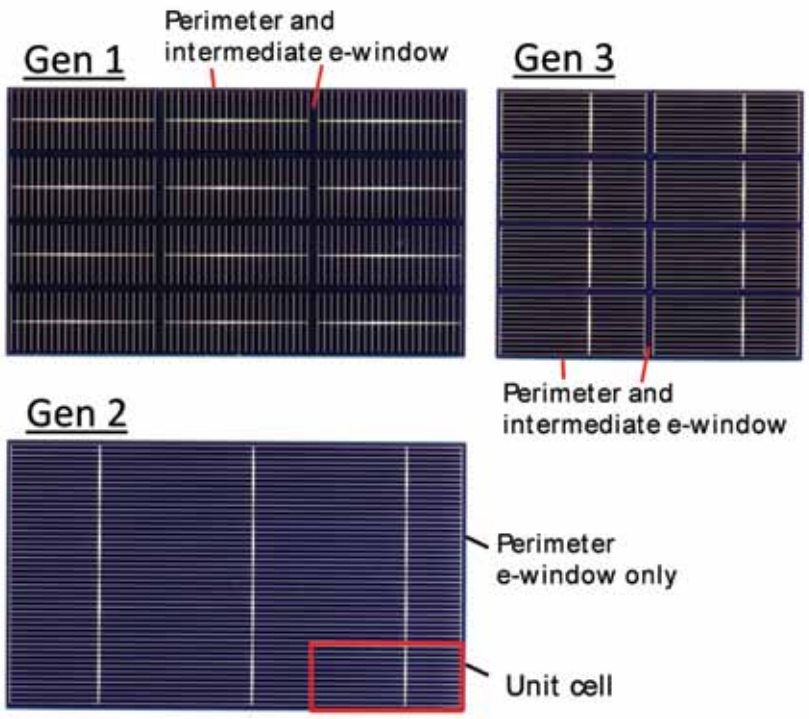

Figure 6. Individualized AP-MWT cells throughout all generations, optimized for an irradiation of 10 suns. The second generation provides perimeter emitter-windows only, allowing continuous metallization and decreased reflectance losses.

area in each direction. Prior to individualization, a solder resist (not shown) is screen printed on the entire rear side, allowing the full degree of freedom in terms of interconnection. Furthermore, no solder structures are used on the illuminated side, thus reducing any potential shading of the front side.

"The AP-MWT architecture facilitates an efficient cell design that will withstand over two decades of irradiation."

Fig. 2 shows a schematic cross section of the AP-MWT architecture; exclusively industrially available processing technologies – for example Cz-Si p-type silicon bulk material, screen-printing and shallow emitter formation – are taken into account. The AP-MWT architecture facilitates an efficient cell design that will withstand over two decades of irradiation. For $C > 1$, the full-area alloyed aluminium back-surface field (Al-BSF) technology

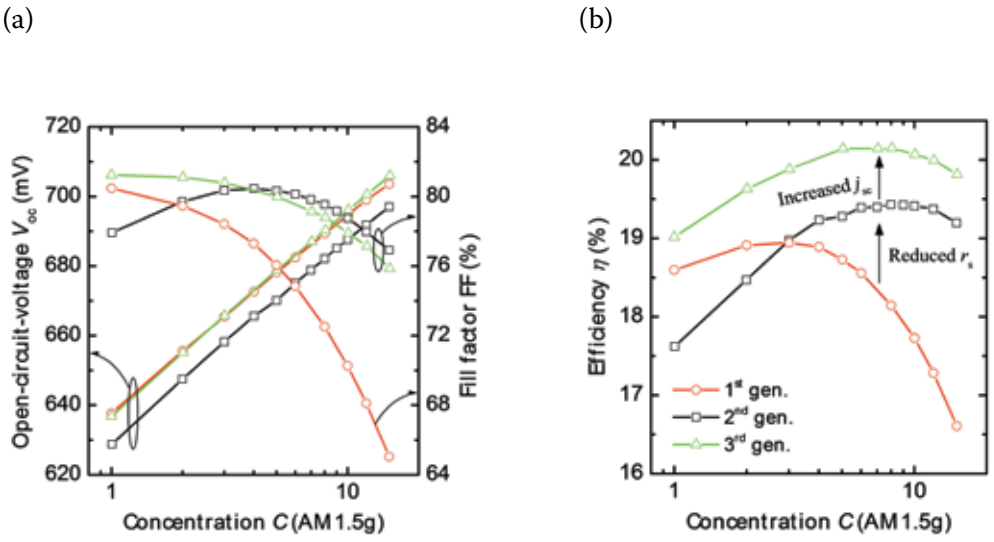

Figure 7. (a) Dependence of V_{oc} and *FF* on the concentration factor; (b) corresponding efficiencies for three selected cells from each generation. According to Equation 1, an efficiency gain can be expected until *FF* losses offset gains in V_{oc}.

	j_{sc} [mA/cm^2]	V_{oc} [mV]	*FF* [%]	η [%]
Mean (10 samples)	39.5±0.1	663±0.7	79.7±0.1	20.9±0.1
Best	39.5	664	79.9	21.0

Table 1. Mean and best value at STC for the AP-MWT cell incorporating PERC technology in accord with the cross section shown in Fig. 2. The *I-V* curves have been recorded 'in-wafer' by applying a mask with an opening of 26.94cm^2, corresponding to the dimensions of format A (see Fig. 1).

is used, providing an efficient contact of virtually no resistance to the semiconductor. For 1 sun, and particularly for low-light conditions, resistive losses are minor; a second technological route – the passivated emitter and rear cell (PERC) approach – therefore offers the potential of higher conversion efficiencies [11].

Impact of illumination conditions on *I-V* curve parameters

The short-circuit current I_{sc} and the respective short-circuit current density j_{sc} are assumed to vary linearly ($j_{sc} = C \cdot j_{sc}^{C=1}$) [13] with the irradiance E_{in}. A possible sublinearity in the case of inversion layer formation [14] or resistance-limited short-circuit current [15] is excluded over the relevant range of concentration factors that are treated here. Therefore, the conversion efficiency η depends only on the product of the open-circuit voltage V_{oc} and the fill factor *FF*:

$$\eta = \frac{j_{sc}}{E_{in}} \cdot V_{oc} \cdot FF \propto V_{oc} \cdot FF \quad (1)$$

In Fig. 3, fill factor losses induced by series and parallel resistance in accordance with the one-diode model are demonstrated. If a series resistance of 0.7Ωcm² is considered (typical for a standard solar cell produced today), at 10 suns this would lead to a drop in *FF* of 30% abs. By contrast, a parallel resistance of 500Ωcm² would be sufficient in order to reduce shunting losses to less than 0.3% abs. This behaviour is explained by the logarithmic dependence of the shunt current and the linear dependence of the external current on the concentration factor. At 1/10 sun, the characteristics are reversed, with the parallel resistance having a dominating influence.

Why MWT solar cells?

Besides the benefits mentioned earlier associated with interconnection and packaging, the MWT approach offers advantages in the case of inhomogeneous irradiance occurring typically at the system level [3]. Fig. 4 shows the front side of an MWT solar cell and a conventional cell which have been partially shaded in order to simulate inhomogeneous irradiance. Compared with the results without masking (homogeneous irradiance), the conventional design shows a significant drop in *FF*, which is attributed to the greater distance between current-collecting busbars located at the edges of the active area. The present experiment shows the inherent drawback of the front-contacted concentrator cell of being limited to a certain extension parallel to the grid fingers. In the direction along the busbar, this effect is enhanced because of the limited width provided by the external contact (busbar) for interconnection. In the case of the MWT approach, narrow pseudo-busbars with a constant pitch transfer collected current to the external contact pads, so there is no dependence on the cell width.

Results for concentrated irradiance

Fig. 5 shows the evolution of the relevant parameters from corresponding illuminated *I-V* curves for three cell generations processed at Fraunhofer ISE. The *I-V* curves were recorded at an irradiance corresponding to C = 10; the reference spectrum corresponds to the global AM 1.5. The efficiency is based on the full illuminated area corresponding to the full cell area – including metallized, perimeter and intermediate emitter window areas – and not just on the designated areas common to concentrator solar cell *I-V* testing.

Out of the three generations, with C = 10, it was possible to achieve median efficiencies of 18.2±0.3% for the first and 19.8±0.15% for the third, with a maximum efficiency of 20.2%. The main improvement in going from the first to the second generation was achieved by rotating the grid approximately 90 degrees (first generation, see Fig. 1), which resulted in a reduction in series resistance from 0.25±0.02 to 0.14±0.04Ωcm². Furthermore, the second generation offers no intermediate emitter windows between the unit cells, thus allowing a continuous metal grid on the front side. With this design, a solution is provided if final cell size is already known.

For the third generation, paste optimizations led to a contact resistivity of 0.3±0.1mΩcm², which equates to a reduced overall variation in the output parameters. A boost in efficiency is mainly related to the use of higher resistive base material, in the range 1.2 to 1.9Ωcm, leading

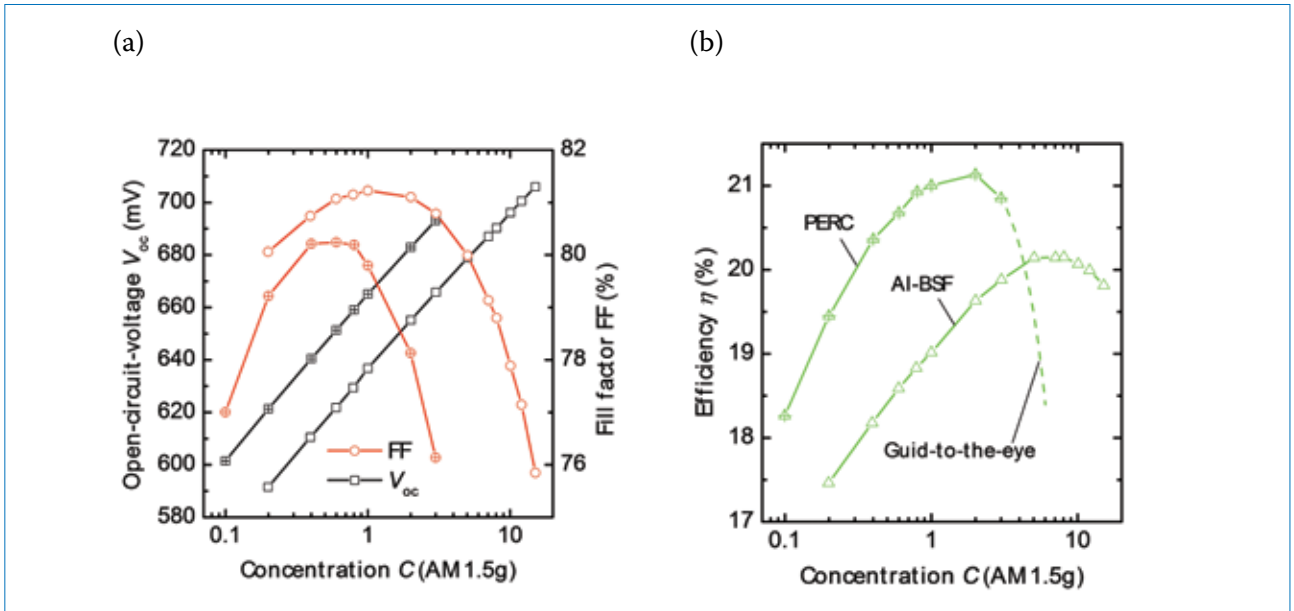

Figure 8. (a) Dependence of V_{oc} and *FF* on the concentration factor; (b) corresponding efficiencies for the AP-MWT PERC (crossed symbols) and Al-BSF (open symbols) devices.

to a significant current gain. Fig. 6 shows a photograph of the front side of the second- and third-generation AP-MWT cells.

"With increasing concentration factor, the reduction of the series resistance associated with minor losses in j_{sc} and V_{oc} is key to maximum performance."

The concentration-dependent *I-V* parameters are shown in Fig. 7 for three representative AP-MWT solar cells from each generation. As a result of the increasing V_{oc}, the efficiency increases accordingly, until the series resistance limits the *FF*. Thus, with increasing concentration factor, the reduction of the series resistance associated with minor losses in j_{sc} and V_{oc} is key to maximum performance.

Results for STC and low-light conditions

With decreasing concentration factor, resistive losses associated with the series resistance of a solar cell decrease accordingly: therefore the PERC approach offers the superior technology in the case of STC and, in particular, low-irradiance conditions.

Table 1 shows *I-V* curve parameters recorded at STC for the AP-MWT architecture incorporating PERC technology. An average conversion efficiency of 20.9%, with a minor standard deviation of 0.1% abs., is reported. The local alloying of Al, on the one hand, provides an efficient contact to the bulk and, on the other, allows a high V_{oc} exceeding 660mV.

Results for different irradiances for AP-MWT PERC and Al-BSF devices are shown in Fig. 8. The front metal grid for the PERC device has been adapted to perform best at STC, whereas the AP-MWT Al-BSF has been optimized for 10 suns. A gap in V_{oc} between the two technologies, mainly attributed to the superior rear side of the PERC device, is observed throughout the range of concentration factors. With increasing concentration, however, the resistive losses start to dominate the *FF*, leading to the superior performance of AP-MWT Al-BSF technology.

The analysis shows the need for adaptions in terms of grid and technological optimizations when the cells are used in varying irradiance. The AP-MWT architecture provides a framework for alternative technological routes in the case of back-contact solar cells, while simultaneously offering a unified interface when it comes to receiver and module assembly.

Receiver and module technology

For reliable and efficient use in the field, the solar cells are assembled in strings and integrated into a receiver or a module. In concentrator applications the receiver protects the active solar cells from environmental influences and allows mounting on the tracking system or other type of fixture. The receiver is the interface to the cooling system, which is crucial in concentrated PV (CPV) systems for efficient operation.

The components and materials of the receiver and module have to be well matched with regard to optical, electrical, thermal and mechanical properties. Because of this requirement, the receiver development becomes a multidisciplinary key task in the entire CPV system.

General receiver description

The receiver concept for AP-MWT cells consists of a generic base profile providing mechanical stability to the cells and allowing the receiver to be easily mounted on any kind of heat sink device. The cells are enclosed in highly transparent encapsulant covered by a glass pane; they are bonded to the base profile by a thin layer of thermally conductive adhesive to enable an efficient thermal management.

Fig 9(a) shows one of the first receivers built and presented at Inter Solar 2013. Fig. 10 shows how the strings are bonded in the aluminium base profile.

The designed receiver can easily be mounted on any kind of active or passive cooling system, enabling it to operate as a PVT (photovoltaic-thermal) absorber for electrical and thermal energy cogeneration. Fig. 11 shows the cross section of a typical design.

"The modules based on AP-MWT architecture developed at ISE exhibit a low serial-resistance loss at the interconnection level and a high packing factor as a result of minimized cell gaps."

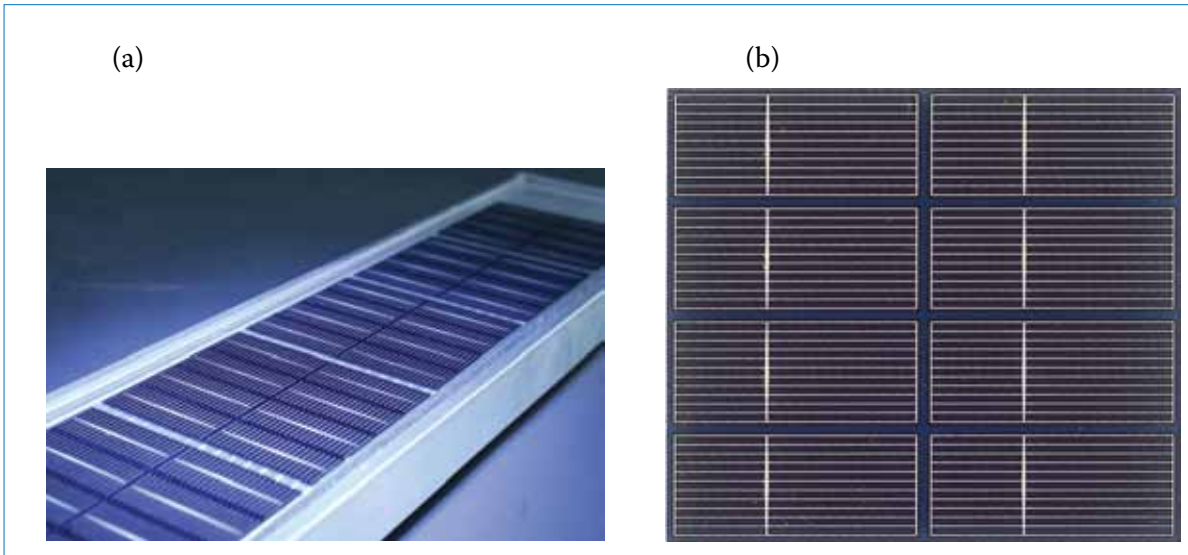

Figure 9. (a) Full string made out of 2 × 4 cells; (b) definition of the X and Y axes in the wafer.

Other than the liquid PDMS (polydimethylsiloxane) silicone encapsulation necessary for CPV applications, the cell and interconnection technology is compatible with low-cost standard EVA lamination or polyurethane encapsulation for 1-sun (or below) applications. The modules based on AP-MWT architecture developed at ISE exhibit a low serial-resistance loss at the interconnection level and a high packing factor as a result of minimized cell gaps. This makes the modules suitable for a large range of applications in which various module formats and specific *I-V* characteristics are required. Because of the high efficiency potential of the MWT cell design, high packing factors and small footprints of the active cell matrix become possible, which is especially beneficial for device integration (see Fig. 12).

Interconnection technology

Solar cell efficiency is maintained at the string and receiver level by the use of an optimized interconnection technology. For AP-MWT architecture, an interconnection concept has been developed in order to suit any cell size extracted from a wafer to full strings. The base interconnector is made of ETP (electrolytic tough pitch) copper foil, which can be adapted to the cell current in order to minimize losses in a concentration range of 1 to 30. The interconnection is designed to keep the resistive power losses below 1% relative to the cell power. The interconnector design is optimized by means of electrical FEM (finite element method) simulations.

Fig. 13 shows, as a function of concentration, the simulated relative power loss for interconnectors of thicknesses 70, 100 and 120µm, for a constant power generation of 0.513W/sun at a current density of 37mA/cm^2 from 1 to 30 suns. The dashed line representing a 1% power loss shows that the 70µm interconnectors are sufficient for applications of less than 5 suns, and that the 100µm interconnectors would carry enough current for values of *C* up to approximately 14. For higher concentration ratios the thickness would need to be adapted accordingly.

Figure 10. Photograph of assisted string handling during receiver production.

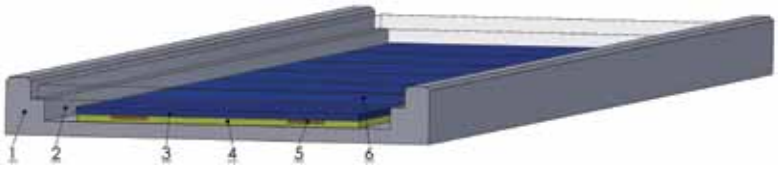

1. Aluminium profile
2. Encapsulation material
3. PV string
4. Thermal adhesive
5. Copper interconnectors
6. Glass cover

Figure 11. Schematic of the layer set-up of a receiver.

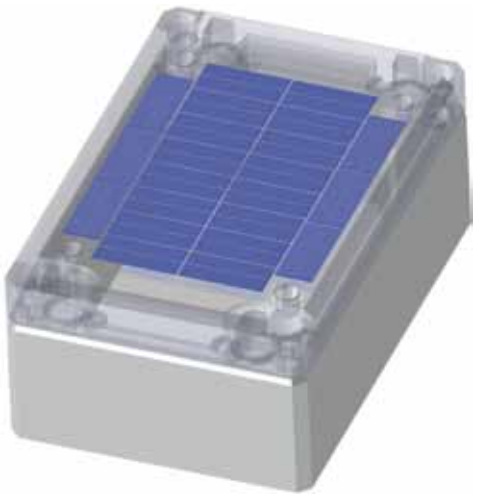

Figure 12. 3-D CAD model of an electronic case with integrated PV module for 1-sun applications.

C	I_{sc} [A]	V_{oc} [V]	P_{mpp} [W]	V_{mpp} [V]	I_{mpp} [A]	*FF* [%]	η [%]	CTM_{PMPP} [%]	CTM_{FF} [%]
1	0.97	4.44	3.50	3.8	0.92	80.8	18.1	99.66	101.1
9.7	9.40	4.87	32.9	3.78	8.7	71.9	17.6	94.6	99.2

Table 2. *I-V* measurement results for receiver at 1 sun and approximately 10 suns (CTM = cell to module).

String layout

Depending on the concentration level and the interconnector thickness (standard is 100µm), the cell length is adapted in order to minimize the resistive losses and to maximize the string efficiency. The results of the FEM calculation are fed into an electrical string model, to determine the optimal cell size for a given cell gap as a function of the concentration level, as shown in Fig. 14.

The cell width is a multiple of the unit cell width and is therefore independent of the concentration level, as each unit cell has its own interconnector path. The resulting characteristic curve allows the cell length to be chosen and the string to be designed, depending on the desired concentration level.

Performance results

Table 2 shows the *I-V* results of a prototype receiver with first-generation cells. The receiver is characterized from 1 to 20 suns using a sun simulator under non-calibrated conditions. The short-circuit current measured for 1 sun under calibrated conditions is used to determine the effective concentration at the cell level for the concentrated measurements. The *I-V* data is measured using a flash simulator with a 1ms intensity plateau. Two *I-V* curves are recorded during two consecutive flashes: the module voltage is switched from I_{sc} to V_{oc} during the first flash, and from V_{oc} to I_{sc} during the second. The comparatively short measurement time leads to the occurrence of hysteresis effects [16] between these two *I-V* curves, mainly affecting the fill factor. Because of these effects, the *FF* reported here might vary from ±1.8% to ±0.8% relative to the true value, with a tendency for this variation to decrease with increasing concentration. The results shown in Table 2 correspond to the mean values of the two recorded *I-V* curves.

The measurement results are shown in Fig. 15 for different concentrations. The calculated efficiency is related to the string area, which consists of the net cell area plus a gap of 1.2mm between the cells, corresponding to a packing factor of 97.5%.

The cell-to-module (CTM) ratio for the maximum power is 94.6% at ~10 suns and 99.66% at 1 sun (Table 2); this ratio takes into consideration all the losses caused by receiver integration, such as interconnection and encapsulation. The CTM ratio for the fill factor is 99.2% at ~10 suns and 101.1% at 1 sun; these high CTM fill-factor ratios demonstrate the high interconnection efficiency in the presented concept. The fill factor CTM ratio gain (> 100%) at 1 sun is related to the reduced current in the receiver (as a result of mismatch effects and optical losses) compared with the initial cell currents. This leads to a reduced impact of the serial resistance and to an increase in fill factor.

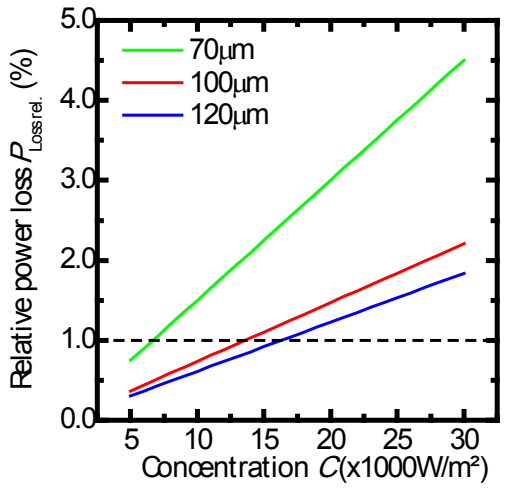

Figure 13. Calculated relative power loss for three different interconnector copper thicknesses as a function of concentration *C*.

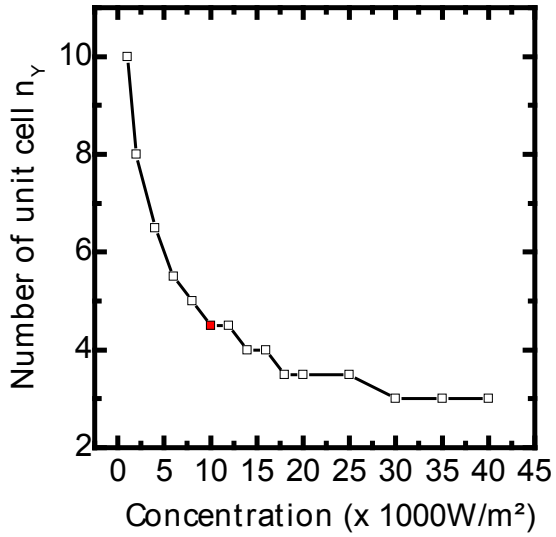

Figure 14. Theoretical optimal number of unit cells n_Y in the Y direction (see Fig. 9(b)), in relation to string efficiency, as a function of concentration. The red symbol indicates the 10-sun data point.

Conclusion

This paper has presented a highly efficient and versatile cell and receiver technology that is able to serve a large variety of applications, ranging from low-light irradiance conditions to a concentration factor of 25. The all-purpose metal-wrap-through (AP-MWT) architecture combines the MWT cell concept with existing state-of-the-art technologies, such as full-area Al-BSF and PERC, in a unit cell design. Thanks to the flexible design, the perimeter dimensions of a final cell can vary between 2.25 and 189cm², which allows a wide range of current–voltage ratios, offering customized solutions besides the conventional flat-panel market.

"For STC and low-light applications, PERC technology offers a higher potential than Al-BSF, delivering top efficiencies of 21.0% at 1 sun and 18.3% at 1/10 sun."

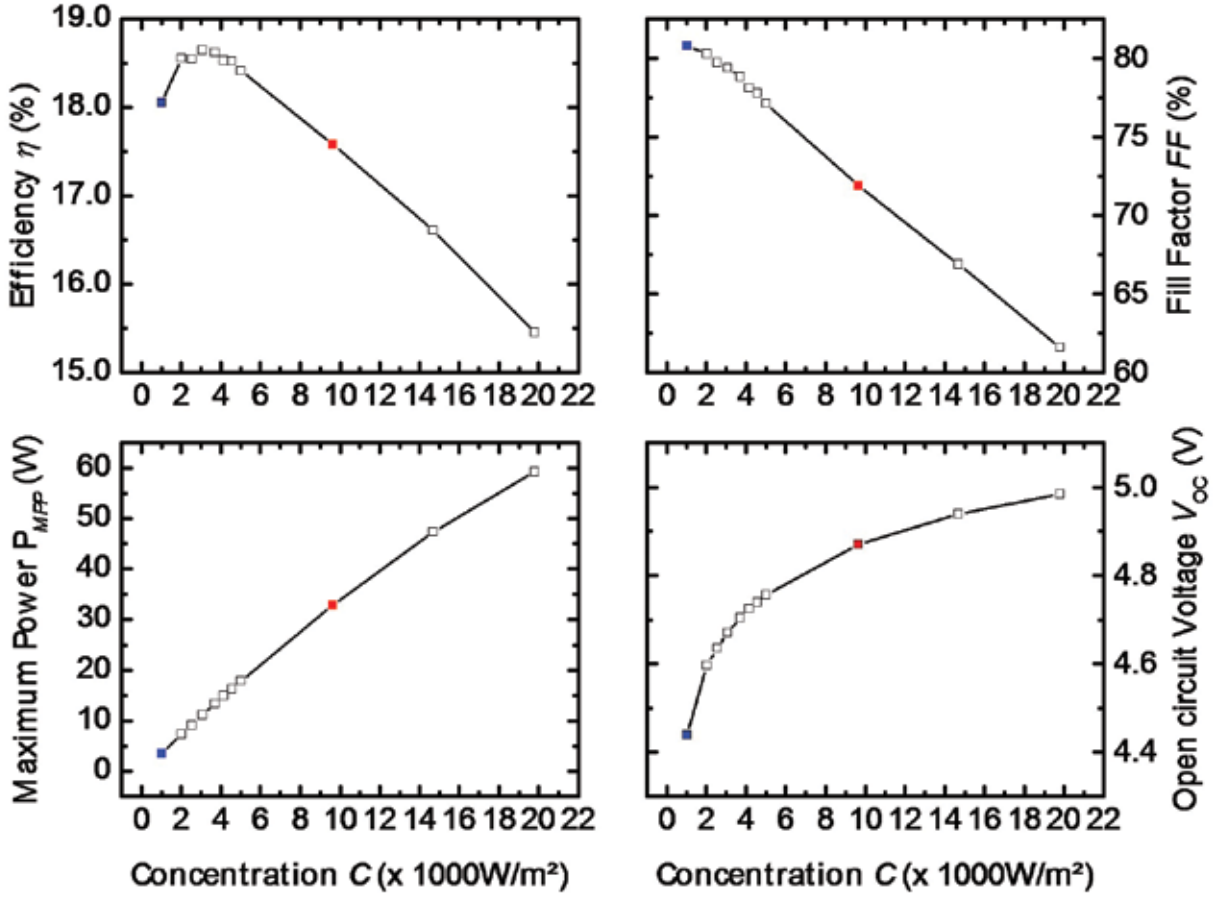

Figure 15. Non-calibrated sun simulator measurements for the receiver for *C* ranging from 1 to 20 (*C* × 1000W/m²). (Blue symbol: 1-sun data point; red symbol: ~10-sun data point.)

The full-area Al-BSF approach allows low series resistances for use beyond concentration factors of 5 suns, resulting in a top efficiency of 20.2% at 10 suns. In contrast, for STC and low-light applications, PERC technology offers a higher potential than Al-BSF, delivering top efficiencies of 21.0% at 1 sun and 18.3% at 1/10 sun.

An interconnection and packaging technology has subsequently been developed that is able to maintain the high power of the cell at the module (1 sun) and receiver (C > 1) levels. A CTM ratio of 94.6% for the maximum power level for 10 suns is reported. This prototype receiver demonstrates that the optical and electrical components harmonize well, transferring the high cell efficiency to a respectable receiver efficiency. The next development step consists of an outdoor evaluation to characterize the thermal behaviour of the receiver.

Acknowledgements

The authors would like to thank the Photovoltaic Technology Evaluation Center team for its support, especially A. Sharaiha, T. Chipei and C. Harmel. Special thanks go to Abengoa SE – our project partner supporting the mutual concentrator activities.

References

[1] SEMI PV Group Europe 2014, "International technology roadmap for photovoltaic (ITRVP): Results 2013", 5th edn (March) [available online at http://www.itrpv.net/Reports/Downloads/].

[2] ISO/IEC 17025:2005, "General requirements for the competence of testing and calibration laboratories".

[3] Luque, A.L. & Viacheslav, A. (Eds) I. 2007, *Concentrator Photovoltaics*. Berlin: Springer.

[4] Spaderna, D.W. & Navon, D.H. 1978, "Solar-cell operation under concentrated illumination", *IEEE Trans. Electron. Dev.*, Vol. ED-25, pp. 1290–1297.

[5] Wenham, S.R. & Green, M.A. 1986, "Laser grooved solar cell", US Patent No. 4,626,613.

[6] Mason, N.B., Bruton, T.M. & Balbuena, M.A. 2002, "Laser grooved buried grid silicon solar cells from pilot line to 50 MWp manufacture in ten years", plenary paper, *Proc. PV in Europe*, Rome, Italy, pp. 227–229.

[7] Vivar, M. et al. 2010, "Laser grooved buried contact cells optimised for linear concentration systems", *Solar Energy Mater. & Solar Cells*, Vol. 94, pp. 187–193.

[8] Slade, A. & Garboushian, V. 2005, "27.6% efficient silicon concentrator solar cells for mass production", *Proc. 20th EU PVSEC*, Barcelona, Spain, pp. 1–2.

[9] Bunea, M.M. et al. 2010, "Simulation and characterization

of high efficiency back contact cells for low-concentration photovoltaics", *Proc. 35th IEEE PVSC*, Honolulu, Hawaii, USA, pp. 000823–000826.

[10] van Kerschaver, E. et al. 1998, "A novel silicon solar cell structure with both external polarity contacts on the back surface", *Proc. 2nd World Conf. PV Solar Energy Conv.*, Vienna, Austria, pp. 1479–1482.

[11] Blakers, A.W. et al. 1989, "23% efficient silicon solar cell", *Proc. 9th EU PVSEC*, Freiburg, Germany, pp. 328–329.

[12] Brooks, R.D. & Mattes, H.G. 1971, "Spreading resistance between constant potential surfaces", *Bell System Tech. J.*, Vol. 50, pp. 775–784.

[13] Reich, N.H. et al. 2009, "Crystalline silicon cell performance at low light intensities", *Solar Energy Mater. & Solar Cells*, Vol. 93, pp. 1471–1481.

[14] Saint-Cast, P. et al. 2012, "A review of PECVD aluminium oxide for surface passivation", *Proc. 27th EU PVSEC*, Frankfurt, Germany, pp. 1797–1801.

[15] Fellmeth, T. 2009, "Entwicklung einer MWT (metal wrap through) Silizium Solarzelle zur Anwendung in niederkonzentrierenden PV-Systemen", Diplomarbeit, Department of Physics, University of Konstanz, Germany.

[16] Lipps, F. 1995, "Vergleich und Modellierung von stationär und transient gemessenen I-U Kennlinien an PV-Modulen", Diplomarbeit, Department of Physics, University of Freiburg, Germany.

About the Authors

Tobias Fellmeth studied physics at the University of Konstanz, Germany, and finished his diploma thesis on concentrator MWT solar cells at Fraunhofer ISE in 2009. Tobias is currently working on silicon-based concentrator solar cells in the final year of his Ph.D. degree.

Matthieu Ebert holds a master's in renewable energy systems from HTW Berlin. In the past he has worked at Fraunhofer ISE in the modules development group and at ANU (Canberra, Australia) on LCPVT projects. Since 2012 he has been working as a scientist within the crystalline photovoltaic modules group at Fraunhofer ISE, where he focuses on new module concepts, such as lightweight module designs and the industrial feasibility of low-concentrating concepts.

Raphael Efinger studied printing technology at the University of Printing and Media in Stuttgart and graduated in 2008. From 2009 to 2011 he worked at Day4 Energy Inc. as a research scientist in the field of cell-to-module integration using the multiwire busbar approach. Since 2012 Raphael has been working as a research engineer at Fraunhofer ISE.

Ingrid Hädrich studied industrial engineering at the technical university in Freiberg, Germany. After finishing her diploma thesis on the optical and thermal evaluation of flat plate crystalline solar modules at Fraunhofer ISE, she worked for two years as a scientist in the crystalline photovoltaic modules group. Since 2010 she has been the head of the module efficiency and new concepts team at Fraunhofer ISE, focusing on alternative module concepts, such as device integrated concepts, BIPV, low concentrating receivers and lightweight modules.

Florian Clement is head of the MWT solar cells and printing technology group at Fraunhofer ISE. He received his Ph.D. in 2009 from the University of Freiburg. Florian's research focuses on the development of highly efficient pilot-line-processed MWT solar cells, as well as on the development and evaluation of printing technologies.

Ulrich Eitner studied technical mathematics at the University of Karlsruhe, Germany. From 2006 to 2011 he worked on the thermomechanics of PV modules at the Institute for Solar Energy Research Hamelin (ISFH) and obtained his Ph.D. from the University of Halle-Wittenberg. Ulrich has been managing the photovoltaic modules group at Fraunhofer ISE since 2011.

Daniel Biro studied physics at the University of Karlsruhe, Germany, and at the University of Massachusetts Amherst, USA. He received his Ph.D. in the field of silicon solar cell diffusion technologies in 2003 from the University of Freiburg. After joining the silicon cell characterization group at Fraunhofer ISE in 1995, Daniel moved to the silicon solar cell production technology group in 1999. He is currently head of the thermal, PVD and printing technology / industrial cell structures department.

Enquiries

Fraunhofer Institute for Solar Energy Systems (ISE)
Heidenhofstrasse 2
79110 Freiburg
Germany

Tel.: +49 (0) 761 4588 5596
Email: info@ise.fraunhofer.de
Website: www.ise.fraunhofer.de